

Incertitudes vibro-acoustiques

dans le domaine transport

Eric Savin

eric.savin@onera.ecp.fr

(+ J.-L. Akian, R. Alexandre, I. Baydoun, **S. Bougacha**,
D. Clouteau, R. Cottreau, **Y. Le Guennec**, **J. Staudacher**)

Onera – Simulation Numérique des Écoulements et Aéroacoustique
29, avenue de la Division Leclerc
F-92322 Châtillon cedex



ECP – Département Mécanique et Génie Civil
Grande Voie des Vignes
F-92295 Châtenay-Malabry



CentraleSupélec

Claims

- The aim is to minimize the efforts required to solve a problem of wave propagation in random media pertaining to structural dynamics and acoustics, *i.e.* perform **waves coarse-graining**.
- Coarse-graining consists in rescaling some phenomena into units or cells or models of size close to the uncertainty of measurement, yielding an **increase of both entropy and dissipation**—hence **irreversibility**.
- The issue is to identify a suitable set of relevant variables for a coarser target level and express them in terms of the variables of a finer source level (in other words rely on **mesoscopic variables** to describe **microscopic scales**).

Outline

- 1 Some issues in structural acoustics
- 2 SEA and ray methods
- 3 Elastic energy transport model
- 4 Numerical examples for slender structures

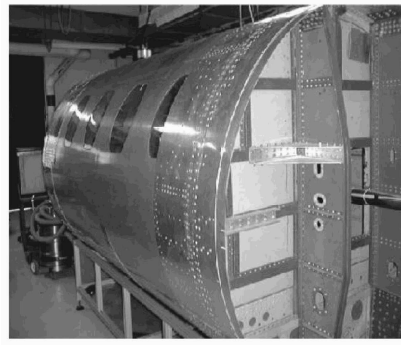
Outline

- 1 Some issues in structural acoustics
- 2 SEA and ray methods
- 3 Elastic energy transport model
- 4 Numerical examples for slender structures

Frequency response function of complex structures

Example #1

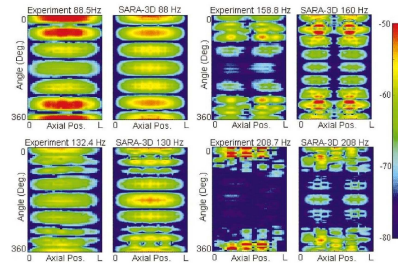
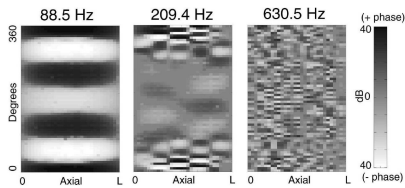
- Cessna Citation fuselage: 9 floor/19 ceiling ribs, 22 stringers.
- Length = 2.55 m, radius = 0.81 m, thickness = 0.8-1.2 mm.



Herdic et al. JASA 117(6) 3667, 2005

Frequency response function of complex structures

Example #1

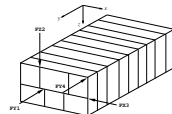
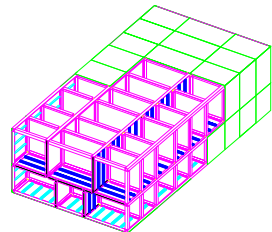


Excitation: point force at a rib/stringer stiffener intersection.

Frequency response function of complex structures

Example #2

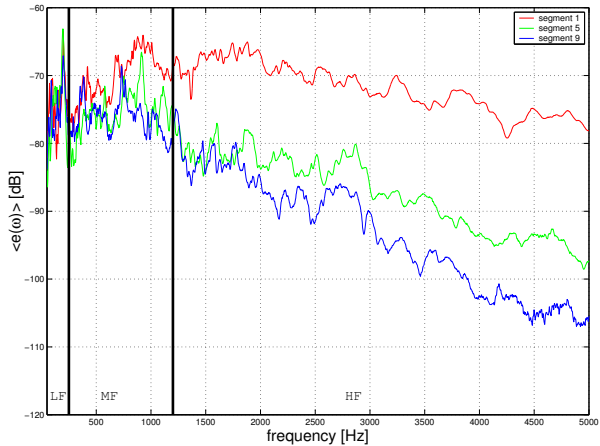
- Complex structure: 200 plates, 400 stiffeners, 54 cavities.
- Length = 5.3 m, width = 2.5 m, height = 1.4 m, mass = 825 kg.



Savin AIAA J. 40(9) 1876, 2002

Frequency response function of complex structures

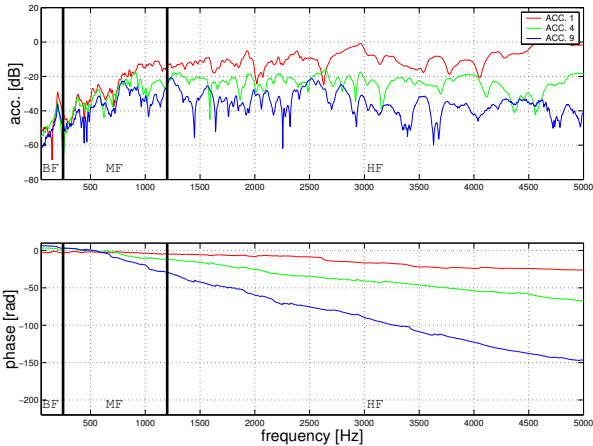
Example #2



Estimated mechanical energies $\mathcal{E} = m\langle v \rangle^2$; $dB_{ref} = 10 \times \log_{10}(1 \text{ kg.m}^2/\text{s}^2)$.

Frequency response function of complex structures

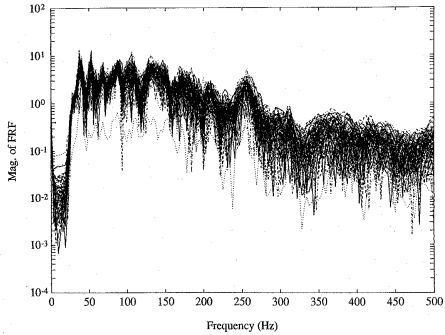
Example #2



Measured vertical accelerations along the structure; $dB_{ref} = 20 \times \log_{10}(1 \text{ m/s}^2)$.

Frequency response function of complex structures

Example #3



Measured FRF amplitudes of 99 "identical" Isuzu Rodeo trucks: acoustic pressure at driver's ear for a mechanical excitation applied to the left front wheel.

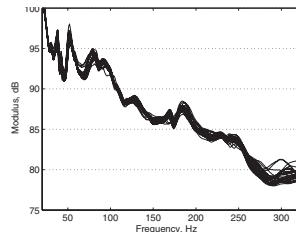
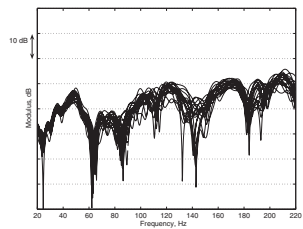
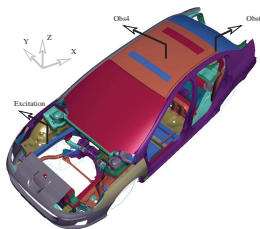
Kompella-Bernhard SAE technical paper #931272, 1993

Kompella-Bernhard NCEJ 44(2) 93, 1996

Wood-Joachim IJVD 8(4-6) 428, 1987

Frequency response function of complex structures

Example #4



Measured structural FRF amplitudes at the back for 20 "identical" PSA cars with different optional extras (middle).

Estimated acoustic energy within the car compartment for 30 different configurations of the same car (right) with $dB_{ref} = 10 \times \log_{10}(2.10^{-5} \text{ Pa})$.

Durand-Soize-Gagliardini JASA 124(3) 1513, 2008

Impulse loads in spatial structures

Example #1: pyrotechnic cut



Impulse loads → High frequency (HF) wave propagation.

Impulse loads in spatial structures

Example #2: solar panel unfolding



Impulse loads → High frequency (HF) wave propagation.

Structural-acoustics system

- **Hypotheses:** linear, visco-elastic materials with density $\rho(\mathbf{x})$ and relaxation tensor $C(\mathbf{x}, t)$, $\mathbf{x} \in \mathcal{O} \subseteq \mathbb{R}^d$, $t \in \mathbb{R}_+$.
- Local **balance of momentum** for the displacement field \mathbf{u} in $\mathcal{O} \times \mathbb{R}$:

$$\rho \partial_t^2 \mathbf{u} = \mathbf{Div} \boldsymbol{\sigma} .$$

- **Constitutive equation** for the stress field $\boldsymbol{\sigma}$ in $\overline{\mathcal{O}} \times \mathbb{R}_+$ as a function of the strain field $\boldsymbol{\epsilon}(\mathbf{u}) = \nabla_{\mathbf{x}} \otimes_s \mathbf{u}$:

$$\boldsymbol{\sigma}(\mathbf{x}, t) = C(\mathbf{x}, 0)\boldsymbol{\epsilon}(\mathbf{u}) + \underbrace{\partial_t C(\mathbf{x}, \cdot) *_t \boldsymbol{\epsilon}(\mathbf{u})}_{\text{ineffective in the high-frequency limit}} .$$

“High-frequency” setting 1/2

- High frequencies correspond to $\varepsilon \rightarrow 0$ for strongly “ ε -oscillatory” initial conditions:

$$\mathbf{u}_\varepsilon(\mathbf{x}, 0) = \mathbf{u}_\varepsilon^0(\mathbf{x}), \quad \| |\varepsilon \nabla_{\mathbf{x}}| \mathbf{u}_\varepsilon^0 \|_{L^2_{\text{loc}}} < \infty,$$

and:

$$\partial_t \mathbf{u}_\varepsilon(\mathbf{x}, 0) = \mathbf{v}_\varepsilon^0(\mathbf{x}), \quad \| |\varepsilon \nabla_{\mathbf{x}}| \mathbf{v}_\varepsilon^0 \|_{L^2_{\text{loc}}} < \infty.$$

- Example: plane waves, $\varepsilon \equiv (|\mathbf{k}|L)^{-1}$,

$$\mathbf{u}_\varepsilon^0(\mathbf{x}) = \varepsilon \mathbf{A}(\mathbf{x}) e^{\frac{i}{\varepsilon} \mathbf{k} \cdot \mathbf{x}}, \quad \mathbf{v}_\varepsilon^0(\mathbf{x}) = \mathbf{B}(\mathbf{x}) e^{\frac{i}{\varepsilon} \mathbf{k} \cdot \mathbf{x}}.$$

“High-frequency” setting 2/2

- Introduce the **acoustic (Christoffel) tensor Γ** of the medium:

$$\Gamma(\mathbf{x}, \mathbf{k})\mathbf{U} = \varrho(\mathbf{x})^{-1}(C(\mathbf{x}) : \mathbf{U} \otimes \mathbf{k})\mathbf{k}, \quad \mathbf{k} \in \mathbb{R}^d, \quad \mathbf{U} \in \mathbb{R}^n.$$

- The local balance of momentum for the displacement field \mathbf{u}_ε in $\mathcal{O} \times \mathbb{R}_t$ is the **elastic wave equation**:

$$\varrho(\mathbf{x}) (\Gamma(\mathbf{x}, i\varepsilon \nabla_{\mathbf{x}}) - (i\varepsilon \partial_t)^2) \mathbf{u}_\varepsilon = O(\varepsilon),$$

supplemented with (e.g. Neumann or Dirichlet) **boundary conditions** on $\partial\mathcal{O} \times \mathbb{R}_t$.

Some properties of Γ

- Γ is symmetric, real, positive definite (in $\mathcal{O} \times \mathbb{R}^d \setminus \{\mathbf{k} = \mathbf{0}\}$): it has n (possibly r_α -multiple) positive eigenvalues λ_α^2 such that:

$$\lambda_\alpha(\mathbf{x}, \mathbf{k}) = c_\alpha(\mathbf{x}, \hat{\mathbf{k}})|\mathbf{k}|, \quad 1 \leq \alpha \leq n,$$

where $\hat{\mathbf{k}} := \mathbf{k}/|\mathbf{k}|$, and the real eigenvectors $\mathbf{b}_\alpha(\mathbf{x}, \mathbf{k}) = \mathbf{b}_\alpha(\mathbf{x}, \hat{\mathbf{k}})$ can be orthonormalized,

$$\Gamma = \sum_{\alpha=1}^n \lambda_\alpha^2 \mathbf{b}_\alpha \otimes \mathbf{b}_\alpha, \quad \mathbb{I}_n = \sum_{\alpha=1}^n \mathbf{b}_\alpha \otimes \mathbf{b}_\alpha.$$

- **Example:** three-dimensional isotropic medium ($n = d$),

$$\Gamma(\mathbf{x}, \hat{\mathbf{k}}) = c_P^2(\mathbf{x})\hat{\mathbf{k}} \otimes \hat{\mathbf{k}} + c_S^2(\mathbf{x})(\mathbb{I}_d - \hat{\mathbf{k}} \otimes \hat{\mathbf{k}}).$$

Energy and power flow densities

- The **energy density** (real, positive) and the **power flow density** (vector) are:

$$\begin{aligned}\mathcal{E}_\varepsilon(\mathbf{x}, t) &= \frac{1}{2}(\rho|\partial_t \mathbf{u}_\varepsilon|^2 + \boldsymbol{\sigma}_\varepsilon : \boldsymbol{\epsilon}_\varepsilon) = \mathcal{T}_\varepsilon + \mathcal{U}_\varepsilon, \\ \boldsymbol{\pi}_\varepsilon(\mathbf{x}, t) &= -\boldsymbol{\sigma}_\varepsilon \partial_t \mathbf{u}_\varepsilon.\end{aligned}$$

- They satisfy for all *fixed* $\varepsilon \in]0, \varepsilon_0]$ a **conservation equation**:

$$\boxed{\partial_t \mathcal{E}_\varepsilon + \operatorname{div} \boldsymbol{\pi}_\varepsilon = 0}.$$

- What happens when $\varepsilon \rightarrow 0$???**

- For constant coefficients the usual parametrix (where $\Gamma^{\frac{1}{2}} = \sum_\alpha \lambda_\alpha \mathbf{b}_\alpha \otimes \mathbf{b}_\alpha$):

$$\mathbf{u}_\varepsilon(\mathbf{x}, t) = \mathcal{F}_{\mathbf{k} \rightarrow \mathbf{x}}^{-1} \left[\cos \left(t \Gamma^{\frac{1}{2}}(\mathbf{k}) \right) \right] * \mathbf{u}_\varepsilon^0(\mathbf{x}) + \mathcal{F}_{\mathbf{k} \rightarrow \mathbf{x}}^{-1} \left[\Gamma^{-\frac{1}{2}}(\mathbf{k}) \sin \left(t \Gamma^{-\frac{1}{2}}(\mathbf{k}) \right) \right] * \mathbf{v}_\varepsilon^0(\mathbf{x})$$

propagates oscillations of wavelength ε which inhibit (\mathbf{u}_ε) from converging strongly in a suitable sense since Γ is positive.

Energy and power flow densities

- Accounting for dissipation and power inputs, the conservation equation reads (ε fixed):

$$\pi_{\text{inj}} = \partial_t \mathcal{E}_\varepsilon + \operatorname{div} \boldsymbol{\pi}_\varepsilon + \pi_{\text{dis}}.$$

- Integrating on the bounded subdomain $\mathcal{D} \subset \mathcal{O}$ with boundary $\partial\mathcal{D}$ of unit outward normal $\hat{\mathbf{n}}$:

$$\int_{\mathcal{D}} \pi_{\text{inj}} d\mathbf{x} = \int_{\mathcal{D}} (\partial_t \mathcal{E}_\varepsilon + \pi_{\text{dis}}) d\mathbf{x} + \underbrace{\int_{\partial\mathcal{D}} \boldsymbol{\pi}_\varepsilon \cdot \hat{\mathbf{n}} d\gamma}_{= \int_{\mathcal{D}} \operatorname{div} \boldsymbol{\pi}_\varepsilon d\mathbf{x}},$$

owing to the divergence (Green-Ostrogradski) theorem.

Existing approaches for structural-acoustics

Statistical Energy Analysis (SEA)

Westphal 1957, Lyon-Maidanik 1962, Smith 1962, Maidanik 1976 ...

Vibrational conductivity analogy (VCA)

Rybak 1972, Nefske-Sung 1989, Belyaev 1991, Bernhard *et al.* 1992, Langley 1995,
Ichchou-Jézéquel 1996, Vlahopoulos *et al.* 1999, Le Bot 2002.

Existing approaches for structural-acoustics

Ray methods with real phases (WKBJ/FIO)

Carlini 1817, Green 1837, Liouville 1837 [...] Keller 1958, Steele 1969, Pierce 1970, Germogenova 1973, Maslov-Fedoruk 1981, Norris 1995...

Ray methods with complex phases (e.g. Gaussian beams)

Babich 1968, Katchalov-Popov 1981, Červený *et al.* 1982, Ralston 1982, Norris 1988, Tanushev *et al.* 2007...

Kinetic models (applications in geophysics and seismology)

Weaver *et al.* 1990, Campillo-Fink-van Tiggelen *et al.* 1998, Sato-Fehler 1998, Papanicolaou-Ryzhik 1999, Scales *et al.* 2000...

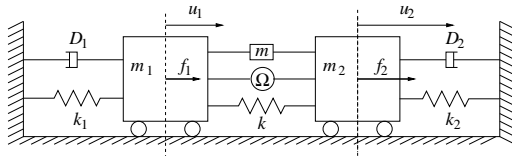
Outline

- 1 Some issues in structural acoustics
- 2 SEA and ray methods
- 3 Elastic energy transport model
- 4 Numerical examples for slender structures

Statistical Energy Analysis 1/3

Model problem

- Introduced in 1957 by Westphal then continued by Heckl, Lyon, Maidanik, Noiseux, Smith, Ungar, etc. (BBN) by the end of the 50's (Apollo program).
- Model problem: 2-dofs system, conservative coupling (see also Rabi oscillations in quantum mechanics).



$$\begin{aligned}\mathbb{E}\{\Pi_{\text{inj},\alpha}(t)\} &= \mathbb{E}\{\Pi_{\text{dis},\alpha}(t)\} + \mathbb{E}\{\Pi_{\alpha\beta}(t)\}, \\ \mathbb{E}\{\Pi_{\alpha\beta}(t)\} &= \omega_\alpha \eta_{\alpha\beta} \mathbb{E}\{\mathcal{E}_\alpha(t)\} - \omega_\beta \eta_{\beta\alpha} \mathbb{E}\{\mathcal{E}_\beta(t)\}, \quad \beta \neq \alpha \in \{1, 2\}.\end{aligned}$$

- $\mathbb{E}\{\cdot\}$ stands for statistical mean or time average or eigenfrequency average.
- $\omega_\alpha \eta_{\alpha\beta} = \omega_\beta \eta_{\beta\alpha}$ where $\eta_{\alpha\beta}$ is the coupling loss factor.

Lyon-Maidanik JASA 34(5) 623, 1962

Statistical Energy Analysis 2/3

\mathcal{N} coupled continuous systems

- SEA assumptions: extension to the conservative, **weak coupling** of \mathcal{N} sub-systems \equiv groups of N_r eigenmodes, $1 \leq r \leq \mathcal{N}$, unchanged by the coupling.
- Then:

$$\mathbb{E}\{\Pi_{\text{inj},r}(t)\} = \underbrace{\mathbb{E}\{\Pi_{\text{dis},r}(t)\}}_{\int_{\mathcal{D}_r} \boldsymbol{\pi}_{\text{inj}} d\mathbf{x}} + \underbrace{\sum_{s \neq r} \mathbb{E}\{\Pi_{rs}(t)\}}_{\int_{\partial \mathcal{D}_r} \boldsymbol{\pi} \cdot \hat{\mathbf{n}} d\gamma},$$

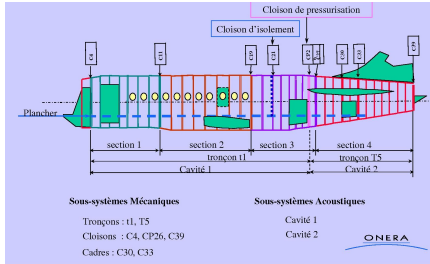
with:

$$\mathbb{E}\{\Pi_{rs}(t)\} \simeq \omega_0 \eta_{rs} \mathbb{E}\{\mathcal{E}_r(t)\} - \omega_0 \eta_{sr} \mathbb{E}\{\mathcal{E}_s(t)\}.$$

- $N_r \eta_{rs} = N_s \eta_{sr}$ where η_{rs} is an average **coupling loss factor**—to be determined!

Statistical Energy Analysis 3/3

Example



- **Input:** modal densities n_r , loss factors η_r , and more difficult, coupling loss factors η_{rs} and input powers $\mathbb{E}\{\Pi_{\text{inj},r}(t)\}$.
- **Output:** average mechanical energies $\mathbb{E}\{\mathcal{E}_r(t)\}$.

Guillaumie-David-Voisin-Grall AST 4(8) 545, 2000

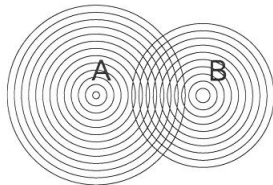
Ray method 1/3

Principles

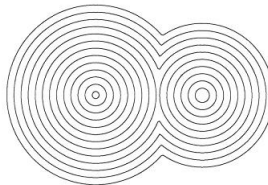
- \mathbf{u}_ε is sought for as a WKBJ ansatz:

$$\mathbf{u}_\varepsilon(\mathbf{x}, t) \simeq e^{\frac{i}{\varepsilon} S(\mathbf{x}, t)} \sum_{k=0}^{\infty} \varepsilon^k \mathbf{U}_k(\mathbf{x}, t).$$

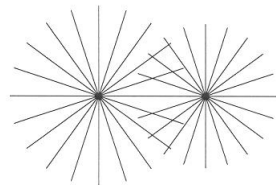
- **Eulerian** point of view (b): the phase S satisfies an **eikonal equation** and the densities $|\mathbf{U}_k|^2$ satisfy **transport equations**.
- **Lagrangian** point of view (c): $(\mathbf{x}, \nabla_{\mathbf{x}} S)$ is given as the solution of the associated Hamiltonian system (**ray tracing**).



(a) Correct solution



(b) Eikonal equation



(c) Ray tracing

Ray method 2/3

Localization of the phase

- Plugging the WKBJ ansatz into the elastic wave equation with $\mathbf{s} = (\mathbf{x}, t) \in \mathcal{O} \times \mathbb{R}$,
 $\xi = (\mathbf{k}, \omega) \in \mathbb{R}^d \times \mathbb{R}$:

$$\mathbf{H}(\mathbf{s}, \nabla_{\mathbf{s}} S) \mathbf{U}_0 = \mathbf{0}, \quad [\text{eikonal}]$$

$$\nabla_{\mathbf{s}} \cdot \left(\mathbf{U}_0^T \nabla_{\xi} \mathbf{H}(\mathbf{s}, \nabla_{\mathbf{s}} S) \mathbf{U}_0 \right) = 0, \quad [\text{transport}]$$

where $\mathbf{H}(\mathbf{s}, \xi) = \varrho(\mathbf{x}) (\Gamma(\mathbf{x}, \mathbf{k}) - \omega^2 \mathbb{I}_n)$ is the dispersion matrix of the medium.

- Thus $\mathcal{H} = \det \mathbf{H} = 0$, but $\mathcal{H}(\mathbf{s}, \xi) = \prod_{\alpha=1}^n \mathcal{H}_{\alpha}(\mathbf{s}, \xi)$ where $\mathcal{H}_{\alpha}(\mathbf{s}, \xi) = \varrho(\mathbf{x}) (\lambda_{\alpha}^2(\mathbf{x}, \mathbf{k}) - \omega^2)$;
therefore:

$$\boxed{\mathcal{H}_{\alpha}(\mathbf{s}, \nabla_{\mathbf{s}} S) = 0}.$$

Ray method 3/3

Shortcomings

- By the divergence theorem applied to the 0-th order transport equation on a ray tube $\tau \mapsto \mathbf{s}(\tau) = (\mathbf{x}(\tau), t(\tau))$ starting from \mathbf{s}_0 :

$$\frac{|\mathbf{U}_0(\mathbf{s}(\tau))|^2}{|\mathbf{U}_0(\mathbf{s}_0)|^2} \propto \frac{q(0)}{q(\tau)},$$

where $q(\tau) = \det(\nabla_{\mathbf{s}_0} \otimes \mathbf{s}(\tau))$, which may cancel on **caustics**.

- The eikonal admits a unique (physical) solution only for sufficiently short times, that happen to be actually very small in highly heterogeneous media.
- When such caustics arise, the WKBJ expansion needs to be generalized as a superposition of propagating fronts; but it is unclear how it can be used to model waves in heterogeneous media.

Research program

- SEA, VCA: approximations (provably wrong);
- Ray methods: superposition principle, regularity... and they give only **one particular** construction of oscillating solutions.

Kinetic models: all oscillating solutions

The key idea: phase space description

(which also accounts for the directions in which waves propagate)

- Mechanical modeling for built-up structures: material heterogeneity and damping, **boundary conditions**, higher-order kinematics;
- Numerical simulations;
- (Further modeling: diffusion limits).

Outline

- 1 Some issues in structural acoustics
- 2 SEA and ray methods
- 3 Elastic energy transport model
- 4 Numerical examples for slender structures

Kinetic modeling

Reversible system

- Consider the bicharacteristic strip $\tau \mapsto (\mathbf{s}(\tau), \xi(\tau))$ as the paths in phase space of some energy "particles" of which density is denoted by $W(\mathbf{s}(\tau), \xi(\tau))$, the latter shall satisfy:

$$\boxed{\frac{dW}{d\tau} = \{\mathcal{H}, W\} = 0} , \quad [\text{TE}]$$

where $\{f, g\} = \nabla_{\xi} f \cdot \nabla_{\mathbf{s}} g - \nabla_{\mathbf{s}} f \cdot \nabla_{\xi} g$ (Poisson bracket).

- But $\frac{d\omega}{d\tau} = 0$ and $\mathbf{H} = \sum \mathcal{H}_\alpha \mathbf{b}_\alpha \otimes \mathbf{b}_\alpha$ with $\mathbb{I}_n = \sum \mathbf{b}_\alpha \otimes \mathbf{b}_\alpha$, thus:

$$\boxed{W = \sum_{\alpha=1}^n w_\alpha \delta(\mathcal{H}_\alpha)} .$$

- The link between W and the sequence (\mathbf{u}_ε) is established by the [Wigner measure](#) of the latter.

Kinetic modeling

Irreversible system

- GENERIC framework:

$$\frac{dW}{d\tau} = \{\mathcal{H}, W\} + [\mathcal{S}, W] = 0, \quad [\text{ITE}]$$

where \mathcal{S} is the **entropy** in this W -system and $[\mathcal{S}, W]$ is the (positive) **dissipative bracket**, both satisfying the degeneracy conditions:

$$\{\mathcal{S}, W\} = [\mathcal{H}, W] = 0.$$

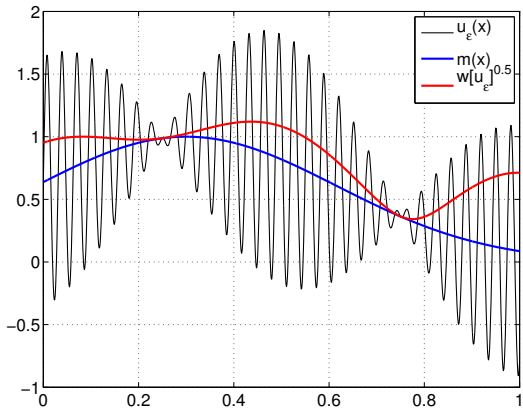
- The link between W and the sequence (\mathbf{u}_ε) is established by the Wigner measure of the latter considering the wave equation with a **time-dependent acoustic tensor**.

Grmela-Öttinger PRE 56(6) 6620, 1997

Öttinger-Grmela PRE 56(6) 6633, 1997

Öttinger, *Beyond Equilibrium Thermodynamics*, Wiley, 2005

Why quadratic observables?

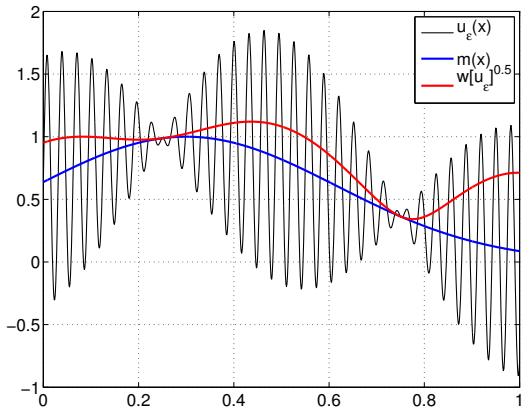


- Let:

$$u_\varepsilon(x) = m(x) + \sigma(x) \sin \frac{x}{\varepsilon},$$

then $(u_\varepsilon) \rightharpoonup m$ weakly in $L^2(\mathbb{R})$ as $\varepsilon \rightarrow 0$, but (u_ε) has no strong limit.

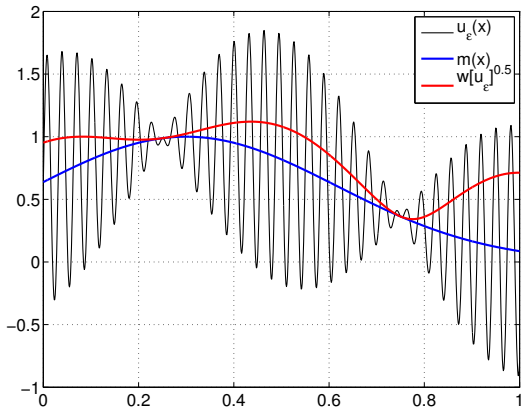
Why quadratic observables?



- Now for any observable $\varphi \in \mathcal{C}_0(\mathbb{R})$:

$$\lim_{\varepsilon \rightarrow 0} (\varphi(x)u_\varepsilon, u_\varepsilon)_{L^2} = \int_{\mathbb{R}} \varphi(x) \left((m(x))^2 + \frac{1}{2}(\sigma(x))^2 \right) dx.$$

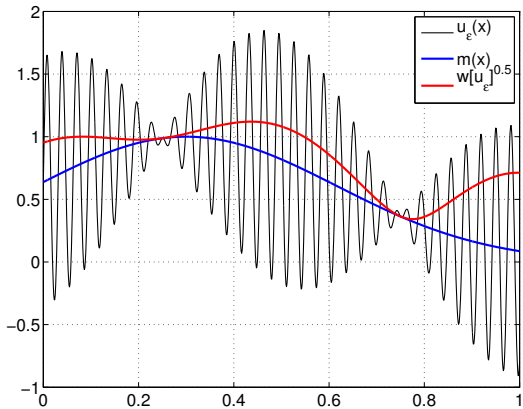
Why quadratic observables?



- Take an observable of the form:

$$\varphi(x, \partial_x) u_\varepsilon(x) = \frac{1}{2\pi} \int_{\mathbb{R}} e^{ik \cdot x} \varphi(x, ik) \hat{u}_\varepsilon(k) dk.$$

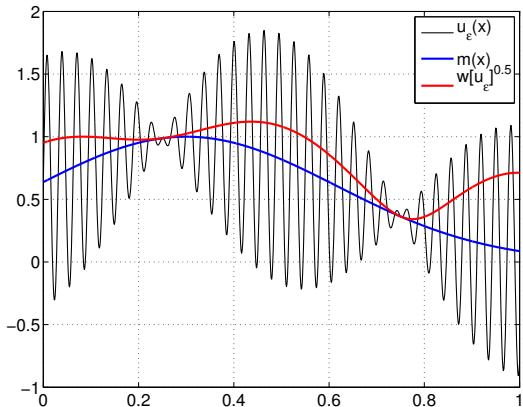
Why quadratic observables?



- Take an observable of the form:

$$\varphi(x, \varepsilon \partial_x) u_\varepsilon(u) = \frac{1}{2\pi} \int_{\mathbb{R}} e^{ik \cdot x} \varphi(x, i\varepsilon k) \widehat{u}_\varepsilon(k) dk.$$

Why quadratic observables?



- Then:

$$\lim_{\varepsilon \rightarrow 0} (\varphi(x, \varepsilon \partial_x) u_\varepsilon, u_\varepsilon)_{L^2} = \iint_{\mathbb{R}^2} \varphi(x, ik) W[u_\varepsilon](dx, dk),$$

where $W[u_\varepsilon]$ is the (positive) **Wigner measure** of (u_ε) .

Wigner measure

Example

- **Example:** the overall kinetic and strain energy densities are in the high-frequency limit $\varepsilon \rightarrow 0$

$$\lim_{\varepsilon \rightarrow 0} \mathcal{T}_\varepsilon(\mathbf{x}, t) = \frac{1}{2} \varrho(\mathbf{x}) \int_{\mathbb{R}^d} \text{Tr } \mathbf{W}[\varepsilon \partial_t \mathbf{u}_\varepsilon(\cdot, t)](\mathbf{x}, d\mathbf{k}),$$

$$\lim_{\varepsilon \rightarrow 0} \mathcal{U}_\varepsilon(\mathbf{x}, t) = \frac{1}{2} \varrho(\mathbf{x}) \int_{\mathbb{R}^d} \boldsymbol{\Gamma}(\mathbf{x}, \mathbf{k}) : \mathbf{W}[\mathbf{u}_\varepsilon(\cdot, t)](\mathbf{x}, d\mathbf{k}),$$

(eventually one can prove that they are equal in this very limit), or

$$\boxed{\lim_{\varepsilon \rightarrow 0} \mathcal{E}_\varepsilon(\mathbf{x}, t) = \sum_{\alpha=1}^n \int_{\mathbb{R}^d} w_\alpha(\mathbf{x}, t; d\mathbf{k})}.$$

Boundary conditions

Rankine-Hugoniot condition

- Let a **discontinuity front** Σ_D be defined by the hypersurface in phase space:

$$\Sigma_D = \{(\mathbf{s}, \boldsymbol{\xi}) \in T^*(\mathcal{O} \times \mathbb{R}); \Sigma(\mathbf{s}, \boldsymbol{\xi}) = 0\}.$$

- The **Rankine-Hugoniot condition** associated to piecewise continuous (weak) solutions of the Liouville equation [TE] on $\Sigma_D \cap \{\mathcal{H}(\mathbf{s}, \boldsymbol{\xi}) = 0\}$:

$$\llbracket \{\mathcal{H}, \Sigma\} W \rrbracket = 0.$$

- Consequence:** continuity of the overall normal power flow across any fixed interface $\{\Sigma(\mathbf{x}, \mathbf{k}) = 0\}$,

$$\sum_{\alpha=1}^n \llbracket \{\lambda_\alpha, \Sigma\} w_\alpha \rrbracket = 0.$$

Boundary conditions

Reflection/transmission coefficients

- $\{\mathcal{H}, \Sigma\} > 0$: transverse reflections (the hyperbolic set);
- $\{\mathcal{H}, \Sigma\} < 0$: total reflections (the elliptic set);
- $\{\mathcal{H}, \Sigma\} = 0$: critical reflections (the glancing set):
 - ▶ $\{\mathcal{H}, \{\mathcal{H}, \Sigma\}\} > 0$: diffractive rays,
 - ▶ $\{\mathcal{H}, \{\mathcal{H}, \Sigma\}\} < 0$: gliding rays,
 - ▶ $\{\mathcal{H}, \{\mathcal{H}, \Sigma\}\} = 0$: higher-order gliding rays (w. inflection point).
- For **elastic waves** the situation is a mix of all cases!
- Boundary conditions raise profound mathematical issues, mostly unsolved to date.
Unfortunately they have also great engineering relevance!

Miller JMPA 79(3) 227, 2000

Savin IMMIJ 1(1) 53, 2007

Le Guennec-Savin JASA 130(6) 3706, 2011

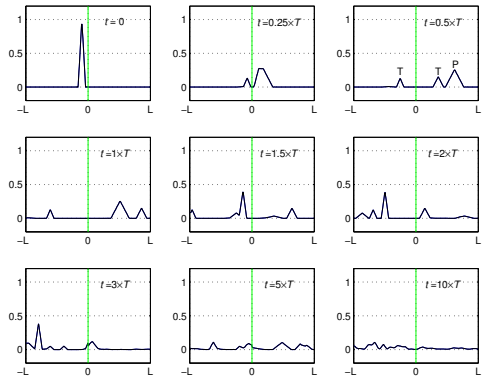
Akian-Alexandre-Bougacha KRM 4(3) 589, 2011

Akian ASY 78(1–2) 37, 2012

Outline

- 1 Some issues in structural acoustics
- 2 SEA and ray methods
- 3 Elastic energy transport model
- 4 Numerical examples for slender structures

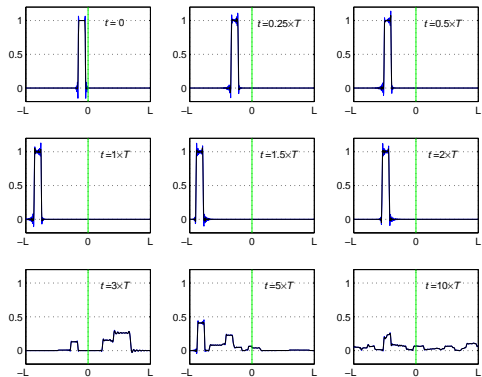
Example #1: beam junction



Runge-Kutta discontinuous FEM
w. Legendre modal expansion
 $\mathcal{N} = 40$, $N = 10$, RK-SSP(8, 8)
— unfiltered
— 1st-order exponential filter

Energy transport in a beam junction with $\phi = 60^\circ$, $\frac{E_2}{E_1} = 2$, $\nu_1 = \nu_2 = 0.3$, and $T = \frac{L}{c_{T2}}$.

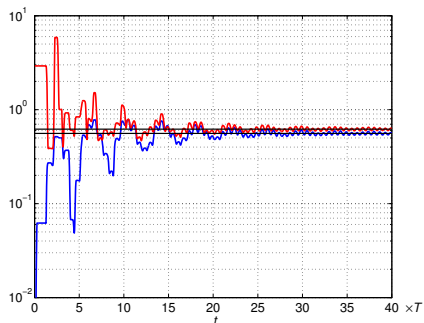
Example #1: beam junction



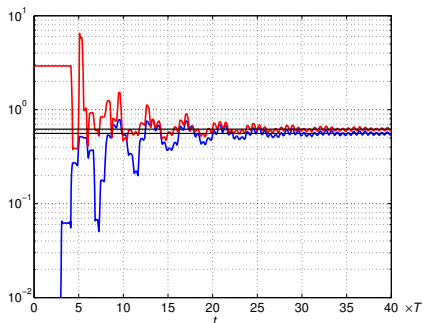
Runge-Kutta discontinuous FEM
w. Gauss-Lobatto nodal expansion
 $\mathcal{N} = 40$, $N = 10$, RK-SSP(8, 8)
— unfiltered
— 0th-order exponential filter

Energy transport in a beam junction with $\phi = 60^\circ$, $\frac{E_2}{E_1} = 2$, $\nu_1 = \nu_2 = 0.3$, and $T = \frac{L}{c_{T_2}}$.

Example #1: beam junction



"Hat" source: Legendre modal expansion
 $\mathcal{N} = 40, N = 5$, RK-SSP(5, 4)

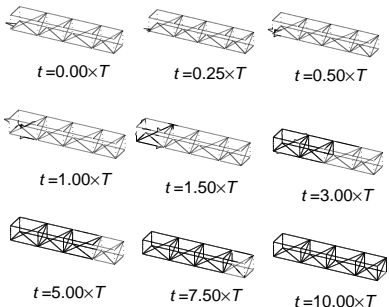


"Square" source: nodal expansion
 $\mathcal{N} = 40, N = 5$, RK-SSP(5, 4)

Energy ratios $t \mapsto \frac{\mathcal{E}_P(t)}{\mathcal{E}_T(t)}$ within each sub-structure (— beam #1, — beam #2); $\phi = 60^\circ$, $\frac{E_2}{E_1} = 2$,
 $\nu_1 = 0.4$, $\nu_2 = 0.1$, $T = \frac{L}{c_{T2}}$.

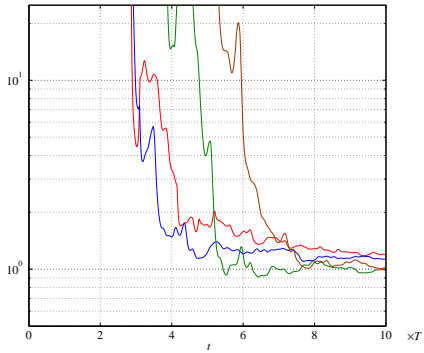
Savin PEM 28 194, 2012

Example #2: beam truss



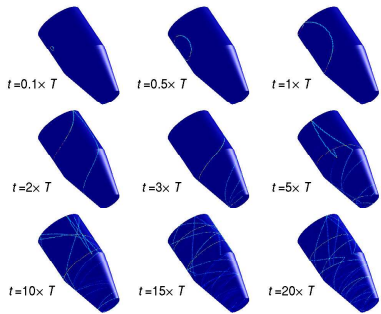
Runge-Kutta discontinuous FEM
w. Legendre modal expansion
 $\mathcal{N} = 1212$, $N = 8$, RK-SSP(8,8) (CFL = 10^{-2})

Energy transport in a beam truss with $T = \frac{L}{c_T}$.

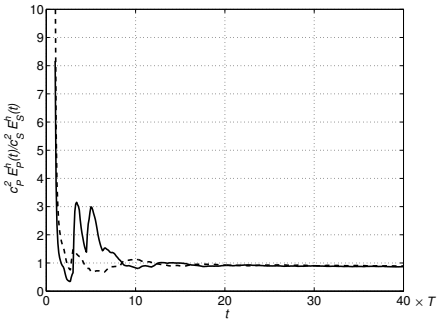


$$\frac{\mathcal{E}_T^r(t)}{\mathcal{E}_P^r(t)} \xrightarrow[t \rightarrow +\infty]{} \frac{2c_P}{c_T} \quad (1 \leq r \leq 4)$$

Example #3: shell junction



Direct Monte-Carlo method
 10^6 sample paths

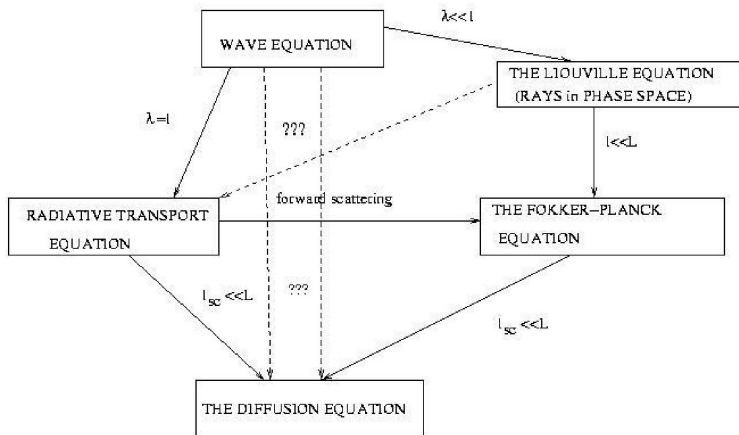


Energy transport in a shell junction impacted by a shear load with $\phi = 15^\circ$, $\frac{E_2}{E_1} = 2$, $\nu_1 = 0.3$,
 $\nu_2 = 0.2$, $T = \frac{L}{c_{T2}}$.

Savin PEM 28 194, 2012

Wave propagation in heterogeneous media

- **Scales:** λ – wavelength, ℓ – correlation length, L – propagation/observation distance...



... and the **mesoscopic scale** ℓ_{sc} – scattering mean free path.

Ryzhik HFWP'05, 2005

Hot topics!

- RTN HYKE 2002–2005, GdR CHANT, GdR Mésolm@ge, GdR Ondes, GdR Ultrasons, ERC StG NuSiKiMo, ANR MNEC...
- CIRM'05, HFNP'05, Waves'07, Waves'09, HYKE'10, Waves'11, HYP'12, Euromech 540...
- AA, CiCP, CiMP, CiMS, JASA, JCP, JHDE, JMP, JSC, **KRM**, WM, WRCM...

